

Structural investigation and electrochemical behaviour of $\text{Li}[\text{Ni}_x\text{Li}_{(1/3-2x/3)}\text{Mn}_{(2/3-x/3)}]\text{O}_2$ compounds by a simple combustion method

Yong Joon Park*, Young-Sik Hong, Xianglan Wu, Kwang Sun Ryu, Soon Ho Chang

Power Source Device Team, Electronics and Telecommunications Research Institute, 161 Gajeong-dong, Yuseong-gu, Daejeon 305–350, South Korea

Received 7 August 2003; accepted 7 November 2003

Abstract

$\text{Li}[\text{Ni}_x\text{Li}_{(1/3-2x/3)}\text{Mn}_{(2/3-x/3)}]\text{O}_2$ ($x = 0.17, 0.25, 0.33, 0.5$) compounds have been prepared by a simple combustion method. Compared with the mixed hydroxide or sol–gel method, the combustion method is very simple, and will therefore reduce the manufacturing cost of the cathode material. The structural and electrochemical properties of the samples were investigated using X-ray diffraction spectroscopy (XRD) and the galvanostatic charge–discharge method. Rietvelt analysis of the XRD patterns shows that these compounds can be classified as α - NaFeO_2 structure type. Compounds with high Ni content ($x = 0.25$ – 0.5 in $\text{Li}[\text{Ni}_x\text{Li}_{(1/3-2x/3)}\text{Mn}_{(2/3-x/3)}]\text{O}_2$) appear to be composed of two phases, namely Ni-rich and Ni-deficient phases with the same α - NaFeO_2 structure. By contrast, the $\text{Li}[\text{Ni}_{0.17}\text{Li}_{0.22}\text{Mn}_{0.61}]\text{O}_2$ compound with a low Ni content has good phase integrity with only a single phase. The initial charge–discharge and irreversible capacity become larger as x in $\text{Li}[\text{Ni}_x\text{Li}_{(1/3-2x/3)}\text{Mn}_{(2/3-x/3)}]\text{O}_2$ decreases. The $\text{Li}[\text{Ni}_{0.50}\text{Mn}_{0.50}]\text{O}_2$ compound has a relatively low initial discharge capacity of 200 mAh g^{-1} and exhibits a large loss in capacity during cycling. On the other hand, $\text{Li}[\text{Ni}_{0.17}\text{Li}_{0.22}\text{Mn}_{0.61}]\text{O}_2$ and $\text{Li}[\text{Ni}_{0.25}\text{Li}_{0.17}\text{Mn}_{0.58}]\text{O}_2$ compounds give high initial discharge capacities of over 245 mAh g^{-1} and a stable cycle performance in the voltage range 4.8 – 2.0 V . The XRD and electrochemical results suggest that the simple combustion method is more appropriate for synthesizing $\text{Li}[\text{Ni}_x\text{Li}_{(1/3-2x/3)}\text{Mn}_{(2/3-x/3)}]\text{O}_2$ compounds with low Ni content.

© 2003 Elsevier B.V. All rights reserved.

Keywords: Cathode; Layered structure; Lithium battery; Combustion method; Capacity

1. Introduction

At present, the most widely used commercial cathode material for lithium-ion batteries is LiCoO_2 due to its ease of production, stable electrochemical cycling, and acceptable specific capacity [1–3]. The relatively high cost of cobalt and the lure of large specific capacity have, however, lead to the study of other possible alternatives. An attractive candidate for the cathode material is Mn-based oxide with a layered structure. Unfortunately, all pure or lightly-doped layered forms of LiMnO_2 have been found to transform to a defective spinel-related form on cycling with significant change in voltage profile. This causes capacity fading during cycling [4–9]. It has been suggested [10] that substitution with fixed low-valence cations such as Al^{3+} , Mn^{2+} , and Li^+ or more electro-negative elements such as Co^{3+} , Cr^{3+} , or Ni^{3+} can be effective in hindering the phase transformation. Armstrong et al. [4,5] have

prepared m - LiMnO_2 with a monoclinic structure ($C2/m$ distorted hexagonal structure). The m - LiMnO_2 prepared by an ion-exchange reaction gave a capacity of only 150 mAh g^{-1} , while m - $\text{LiMn}_{0.9}\text{Co}_{0.1}\text{O}_2$ had a stable reversible capacity of 210 mAh g^{-1} between 4.8 and 2.6 V . Other workers have investigated [11–13] $\text{Li}_2\text{Cr}_x\text{Mn}_{2-x}\text{O}_4$ with a layered structure. The $\text{Li}_2\text{Cr}_x\text{Mn}_{2-x}\text{O}_4$ compound delivered a discharge capacity of over 200 mAh g^{-1} and relatively good retention.

Recently, some groups have attempted to stabilize the Mn-based oxide with a layered structure by using a solid solution between Li_2MnO_3 ($\text{Li}[\text{Li}_{1/3}\text{Mn}_{2/3}]\text{O}_2$) and LiMO_2 ($M = \text{Cr, Ni, Co, } \dots$). Paulsen et al. [14] reported that $\text{Li}[\text{Li}_{0.2}\text{Cr}_{0.4}\text{Mn}_{0.4}]\text{O}_2$ can be regarded as a solid solution between Li_2MnO_3 ($\text{Li}[\text{Li}_{1/3}\text{Mn}_{2/3}]\text{O}_2$) and LiCrO_2 . Numata et al. [15,16] investigated a solid-solution of cathode material, $\text{Li}(\text{Co}_{1-x}\text{Li}_{x/3}\text{Mn}_{2x/3})\text{O}_2$ ($0 \leq x \leq 1$) between Li_2MnO_3 ($\text{Li}[\text{Li}_{1/3}\text{Mn}_{2/3}]\text{O}_2$) and LiCoO_2 . Zhonghua Lu et al. [17–21] have analyzed a solid solution between Li_2MnO_3 ($\text{Li}[\text{Li}_{1/3}\text{Mn}_{2/3}]\text{O}_2$) and LiMO_2 ($M = \text{Cr or Ni}$).

$\text{Li}[\text{Ni}_x\text{Li}_{(1/3-2x/3)}\text{Mn}_{(2/3-x/3)}]\text{O}_2$ and $\text{Li}[\text{Cr}_x\text{Li}_{(1/3-x/3)}\text{Mn}_{(2/3-2x/3)}]\text{O}_2$ are derived from $\text{Li}[\text{Li}_{1/3}\text{Mn}_{2/3}]\text{O}_2$ by

* Corresponding author. Tel.: +82-42-860-5516; fax: +82-42-860-6836.
E-mail address: yjpark@etri.re.k (Y.J. Park).

substitution of Li^+ and Mn^{+4} by Ni^{2+} or Cr^{3+} , respectively. When cell containing such oxides was charged to about 4.8 V, it exhibited an irreversible capacity at around 4.5–4.7 V. After the first charge process, the materials can be reversibly cycled with a high capacity of over 200 mAh g^{-1} in the voltage range of 2.0 and 4.8 V. These oxide materials were conventionally prepared by a mixed hydroxide method or sol–gel method. Although, such methods could lead to a homogeneous cation distribution, they require a complex process and involve a high manufacturing cost.

In the present work, a simple combustion method is used for preparing $\text{Li}[\text{Ni}_x\text{Li}_{(1/3-2x/3)}\text{Mn}_{(2/3-x/3)}]\text{O}_2$ ($x = 0.17, 0.25, 0.33, 0.5$) cathode materials. Compared with the mixed hydroxide or sol–gel method, this approach is very simple and will reduce the manufacturing cost of cathode powders. The stoichiometry of $\text{Li}[\text{Ni}_x\text{Li}_{(1/3-2x/3)}\text{Mn}_{(2/3-x/3)}]\text{O}_2$ is determined from the assumption that the transition metals Ni and Mn are in the oxidation states of +2 and +4, respectively. The structure and electrochemical properties of the powder were investigated using X-ray diffraction (XRD) and a charge–discharge method. Considering the results of these analyses, an appropriate composition for the $\text{Li}[\text{Ni}_x\text{Li}_{(1/3-2x/3)}\text{Mn}_{(2/3-x/3)}]\text{O}_2$ compound is suggested.

2. Experimental

$\text{Li}[\text{Ni}_x\text{Li}_{(1/3-2x/3)}\text{Mn}_{(2/3-x/3)}]\text{O}_2$ ($x = 0.17, 0.25, 0.33, 0.5$) was prepared by a simple combustion method from manganese acetate tetrahydrate $[\text{Mn}(\text{CH}_3\text{CO}_2)_2 \cdot 4\text{H}_2\text{O}]$, nickel(II) nitrate hexahydrate $[\text{Ni}(\text{NO}_3)_2 \cdot 6\text{H}_2\text{O}]$, and lithium acetate dihydrate $[\text{CH}_3\text{CO}_2\text{Li} \cdot 2\text{H}_2\text{O}]$. At first, stoichiometric amounts of the materials of Mn, Ni and Li were mixed with distilled water and stirred continuously at 100°C on a hot plate. The precursors were dissolved in distilled water within a few minutes and a viscous gel with a green colour was obtained after evaporation of the excess water. When the resulting gel was fired at about 400°C , a powder which looked like ash was produced by vigorous decomposition of the organic material. The decomposed powder was ground and heated at 500°C for 3 h. The heat-treated powder was re-ground and re-heated at 900°C in air for 10 h. Then, it was poured into a stainless-steel box and quenched at room temperature.

X-ray diffraction data were collected using a Philips X-ray diffractometer in the 2θ range from 15 to 70° with $\text{Cu K}\alpha$ radiation ($\lambda = 1.5406 \text{ \AA}$). The data was refined by the Rietveld method using the Fullprof program. The peak shape was described by a Pseudo-Voigt function. The background level was defined by a polynomial function. For each diffraction pattern, the scale factor, the counter zero point, the peak asymmetry and the unit-cell dimensions were refined in addition to the atomic parameters.

To prepare the positive electrode, 0.4 g of polyvinyl difluoride (Aldrich) was dissolved in about 25 g *N*-methyl-2-pyrrolidone for 1 h and then 4 g of ample powder and 0.6 g

of Super P black (MMM Carbon Co.) were added. After a day of ball-mill grinding, a viscous slurry was coated on an aluminium foil using a doctor blade and a film of uniform thickness was obtained. The film was then dried at 90°C in an oven. The resulting cathode film was hot-pressed at 135°C to increase the tap density. The thickness of the cathode film was about $30 \mu\text{m}$. The electrochemical cell was assembled in a dry room using the above cathode film, lithium, porous polyethylene film and 1 M LiPF_6 solution in 1:1 volume ratio of ethylene carbonate/dimethyl carbonate. Galvanostatic charge–discharge tests were performed with a Toyo charge–discharge system. The test cells were charged to 4.8 V versus Li/Li^+ with a current density of 20 mA g^{-1} , and then discharged to 2.0 V with the same current density. The cycling tests were performed at 21 or 30°C by using an environmental chamber.

3. Results and discussion

3.1. Structural investigation

X-ray diffraction patterns for $\text{Li}[\text{Ni}_x\text{Li}_{(1/3-2x/3)}\text{Mn}_{(2/3-x/3)}]\text{O}_2$ ($x = 0.17, 0.25, 0.33, 0.5$) cathode materials

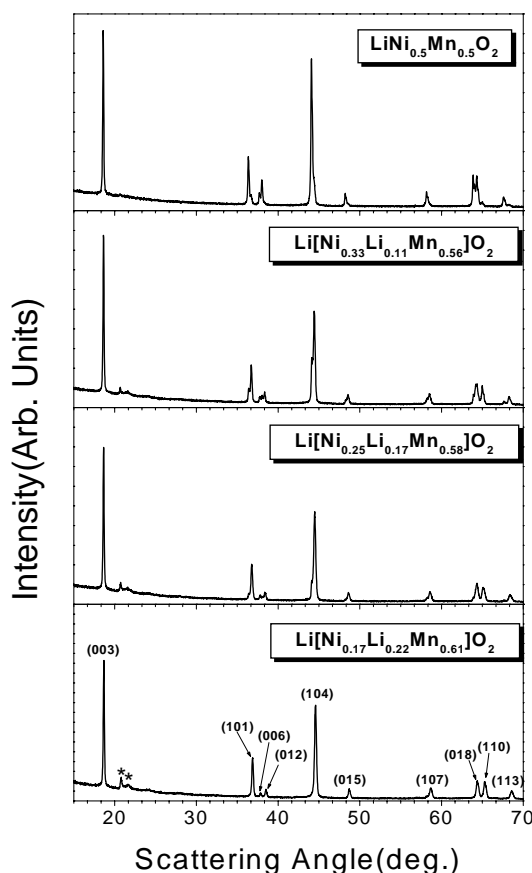


Fig. 1. XRD patterns for $\text{Li}[\text{Ni}_x\text{Li}_{(1/3-2x/3)}\text{Mn}_{(2/3-x/3)}]\text{O}_2$ ($x = 0.17, 0.25, 0.33, 0.5$) compounds prepared at 900°C for 10 h.

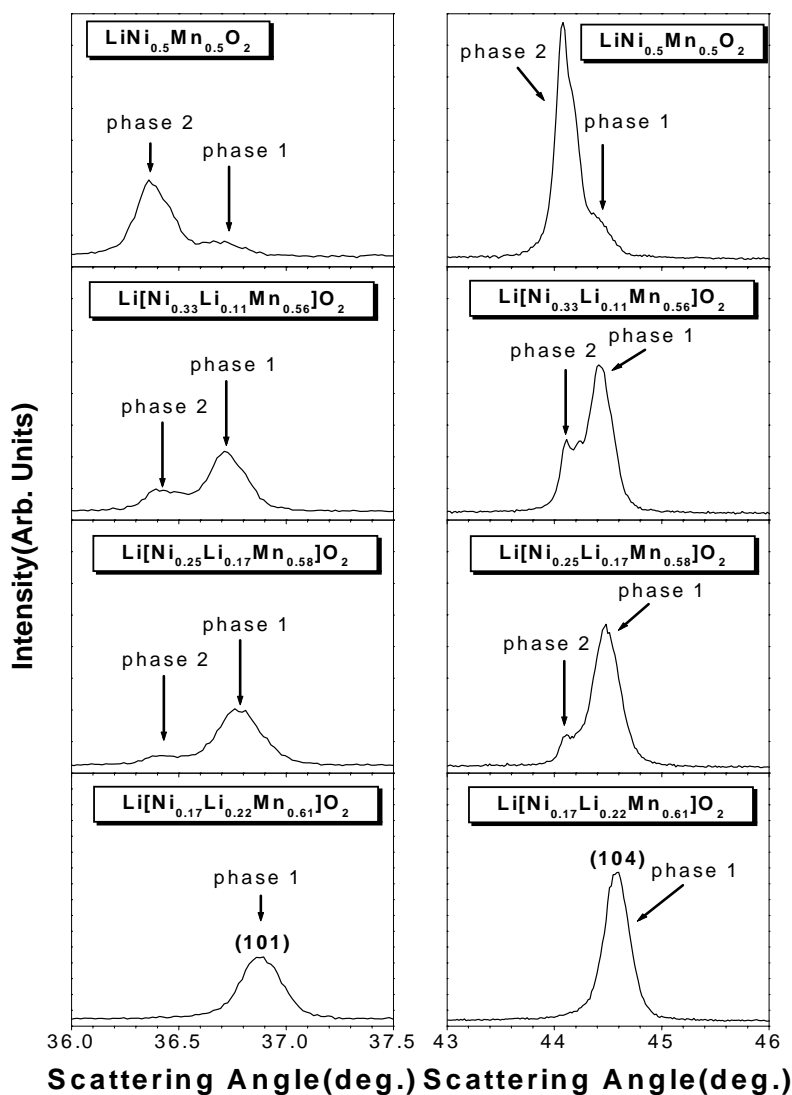


Fig. 2. XRD patterns for $\text{Li}[\text{Ni}_x\text{Li}_{(1/3-2x/3)}\text{Mn}_{(2/3-x/3)}]\text{O}_2$ ($x = 0.17, 0.25, 0.33, 0.5$) compounds enlarged in region $36.0\text{--}37.5^\circ$ and $43.0\text{--}46.0^\circ$.

are shown in Fig. 1. The XRD peaks marked “*” are attributed to the superlattice ordering of Li and Mn in the transition-metal containing layers [17,18]. When the Ni content of the $\text{Li}[\text{Ni}_x\text{Li}_{(1/3-2x/3)}\text{Mn}_{(2/3-x/3)}]\text{O}_2$ compound increases to $x = 0.5$, the superlattice peaks become broad because the scattering contrast between Ni and Mn is much less than that between Li and Mn [18]. Except for the superlattice peaks, most of the peaks can be indexed to a $\alpha\text{-NaFeO}_2$ structure (space group: $R3m$). This is same structure as that of $\text{O}_3\text{-LiCoO}_2$, as found in previous studies [18–21]. Nevertheless, certain peaks of the compounds with high Ni contents split into pairs. The XRD patterns of $\text{Li}[\text{Ni}_x\text{Li}_{(1/3-2x/3)}\text{Mn}_{(2/3-x/3)}]\text{O}_2$ enlarged in the regions $36.0\text{--}37.5^\circ$ and $43.0\text{--}46.0^\circ$ are shown in Fig. 2. There is a splitting of the (101) and (104) peaks for the patterns of $x = 0.25\text{--}0.5$ compounds in the $\text{Li}[\text{Ni}_x\text{Li}_{(1/3-2x/3)}\text{Mn}_{(2/3-x/3)}]\text{O}_2$ series. This indicates that these compounds are composed of two phases, which are named as ‘phase 1’ and ‘phase 2’ for convenience. The $\text{LiNi}_{0.5}\text{Mn}_{0.5}\text{O}_2$

compound has sharp peaks at ‘phase 2’ and broad peaks at ‘phase 1’. with decrease in the Ni content of the compounds, however, the peaks at ‘phase 2’ become smaller and the peaks at ‘phase 1’ become sharper and higher. When the Ni content of the sample decreases to $x = 0.17$, the peaks at ‘phase 2’ are not detected in the XRD pattern.

Rietveld analysis has been performed on the series of compounds to understand the structural properties of the samples. It is assumed that Li is on the 3a sites, Ni^{2+} and Mn^{4+} and Li^+ are on the 3b sites, and the oxygen is on the 6c sites. Since the radius of the Ni^{2+} cation (0.69 \AA) is close to that of Li^+ (0.76 \AA), it is considered that Ni and Li atoms exchange between 3a and 3b sites and that the stoichiometry of the powders is fixed to the nominal values in the Rietveld fitting. The $\text{Li}[\text{Ni}_{0.50}\text{Mn}_{0.50}]\text{O}_2$, $\text{Li}[\text{Ni}_{0.33}\text{Li}_{0.11}\text{Mn}_{0.56}]\text{O}_2$ and $\text{Li}[\text{Ni}_{0.25}\text{Li}_{0.17}\text{Mn}_{0.58}]\text{O}_2$ samples are fitted with a two-phase model.

The XRD pattern of $\text{Li}[\text{Ni}_{0.25}\text{Li}_{0.17}\text{Mn}_{0.58}]\text{O}_2$ is presented in Fig. 3a together with its calculated pattern

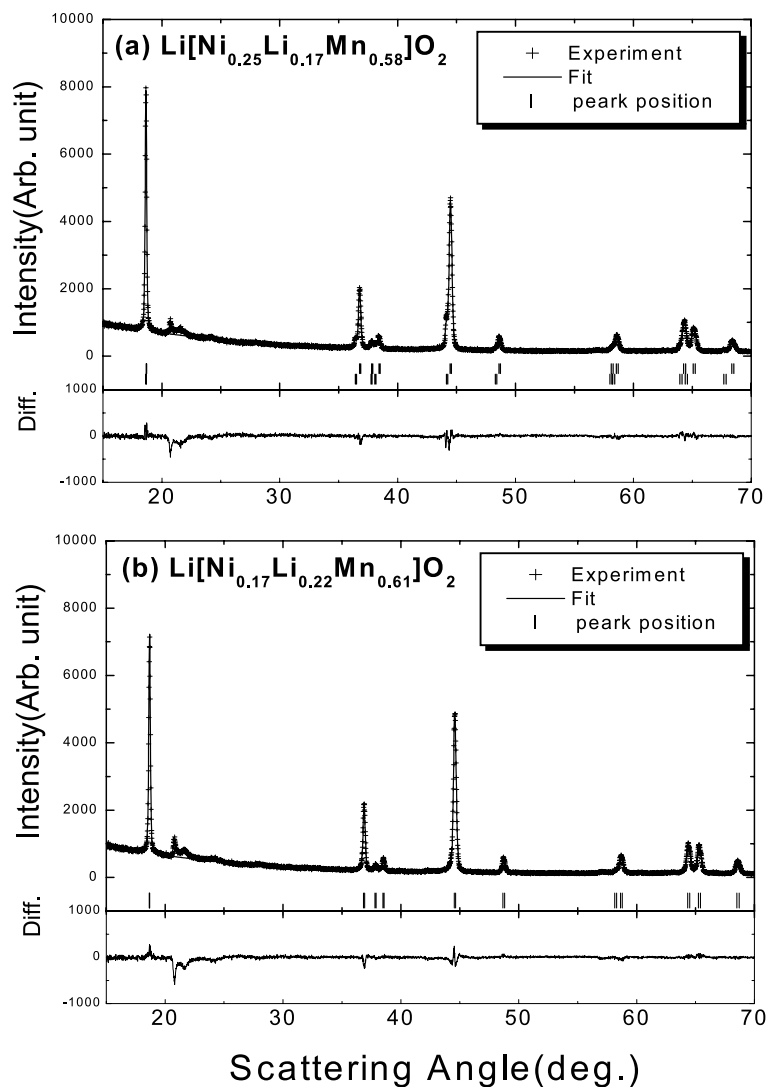


Fig. 3. Experimental XRD patterns and calculated patterns from Rietveld program for (a) $\text{Li}[\text{Ni}_{0.25}\text{Li}_{0.17}\text{Mn}_{0.58}]\text{O}_2$ and (b) $\text{Li}[\text{Ni}_{0.17}\text{Li}_{0.22}\text{Mn}_{0.61}]\text{O}_2$ compounds. Difference between data and calculation is given in lower panel.

based on the Rietveld fit. The samples can be fitted well with two phases; they have the same $\alpha\text{-NaFeO}_2$ structure but different lattice parameter $\text{Li}[\text{Ni}_{0.50}\text{Mn}_{0.50}]\text{O}_2$ and $\text{Li}[\text{Ni}_{0.33}\text{Li}_{0.11}\text{Mn}_{0.56}]\text{O}_2$ samples also can be fitted by the same method. The structural parameters determined by

Rietveld refinement the $\text{Li}[\text{Ni}_x\text{Li}_{(1/3-2x/3)}\text{Mn}_{(2/3-x/3)}]\text{O}_2$ samples are listed in Table 1. Based on the Rietveld analysis, the ‘phase 1’ with a small lattice parameter and the ‘phase 2’ with a large lattice parameter can be interpreted as a Ni-deficient (low x in $\text{Li}[\text{Ni}_x\text{Li}_{(1/3-2x/3)}\text{Mn}_{(2/3-x/3)}]\text{O}_2$

Table 1

Lattice parameters, R factors, and relative percentage determined by Rietveld refinement for $\text{Li}[\text{Ni}_x\text{Li}_{(1/3-2x/3)}\text{Mn}_{(2/3-x/3)}]\text{O}_2$ compounds with $x = 0.17, 0.25, 0.33$ and 0.5

x	Phase	a (Å)	c (Å)	R_p (%)	R_{wp} (%)	R_B (%)	Relative (%)
0.5	1	2.8694(7)	14.2865(8)	20.5	14.5	4.53	12.82
	2	2.8950(8)	14.3132(3)	20.5	14.5	2.40	87.18
0.33	1	2.8703(0)	14.2908(4)	21.1	16.7	2.32	71.35
	2	2.8938(9)	14.3133(5)	21.1	16.7	4.02	28.65
0.25	1	2.8660(0)	14.2829(0)	24.4	19.3	3.57	86.69
	2	2.8928(4)	14.3063(9)	24.4	19.3	5.91	13.31
0.17	1	2.8575(1)	14.2680(7)	26.0	22.4	4.40	100

series) and a Ni-rich (high x in $\text{Li}[\text{Ni}_x\text{Li}_{(1/3-2x/3)}\text{Mn}_{(2/3-x/3)}]\text{O}_2$ series) phase with the same $\alpha\text{-NaFeO}_2$ structure, respectively. The difference in lattice parameter is due to the larger ionic radius of Ni^{2+} (0.69 Å) compared with Mn^{4+} (0.53 Å). The portion of the Ni-deficient phase ('phase 1') is only 12.8% in the compound with a high Ni content of $x = 0.5$, but increases to about 100% in the compound with a low Ni content of $x = 0.17$. As shown in Fig. 3b the entire XRD pattern of $\text{Li}[\text{Ni}_{0.17}\text{Li}_{0.22}\text{Mn}_{0.61}]\text{O}_2$ is fitted well by the $\alpha\text{-NaFeO}_2$ structure with a single phase. The phase-split may be attributed to the inhomogeneous mixing of cations (Ni and Mn) that occurs during the decomposition process of the source materials.

3.2. Electrochemical behaviour

The first three charge–discharge curves for the $\text{Li}[\text{Ni}_x\text{Li}_{(1/3-2x/3)}\text{Mn}_{(2/3-x/3)}]\text{O}_2$ ($x = 0.17, 0.25, 0.33, 0.5$) samples measured at 21 °C are shown in Fig. 4. The

measurements were carried out between 4.8 and 2.0 V using a constant current density of 20 mA g^{-1} (about 0.1 C). Plateaux at about 4.5 V are observed in the first charge profile. The plateaux vanish on subsequent charging and discharging. The voltage profile after the initial charge process is very smooth. The length of the plateaux grows longer as Ni content is decreased.

The initial charge–discharge capacity and irreversible capacity are plotted against the Ni content in Fig. 5. As the content of Ni decreases, both the initial charge and irreversible capacity increase due to an increase of the plateau region. This irreversible plateau has been observed in the initial charge profile of the solid solution between Li_2MnO_3 ($\text{Li}[\text{Li}_{1/3}\text{Mn}_{2/3}]\text{O}_2$) and LiMO_2 ($\text{M} = \text{Cr, Ni, Co, } \dots$) [17–21]. Lu et al. have suggested that irreversible plateaux are due to the simultaneous extraction of both Li and O from the material [18,20]. They assumed that the portion of the first charge to 4.45 V corresponded to de-intercalation of lithium and oxidation of metal ion (Cr, Ni, Co, ...) and

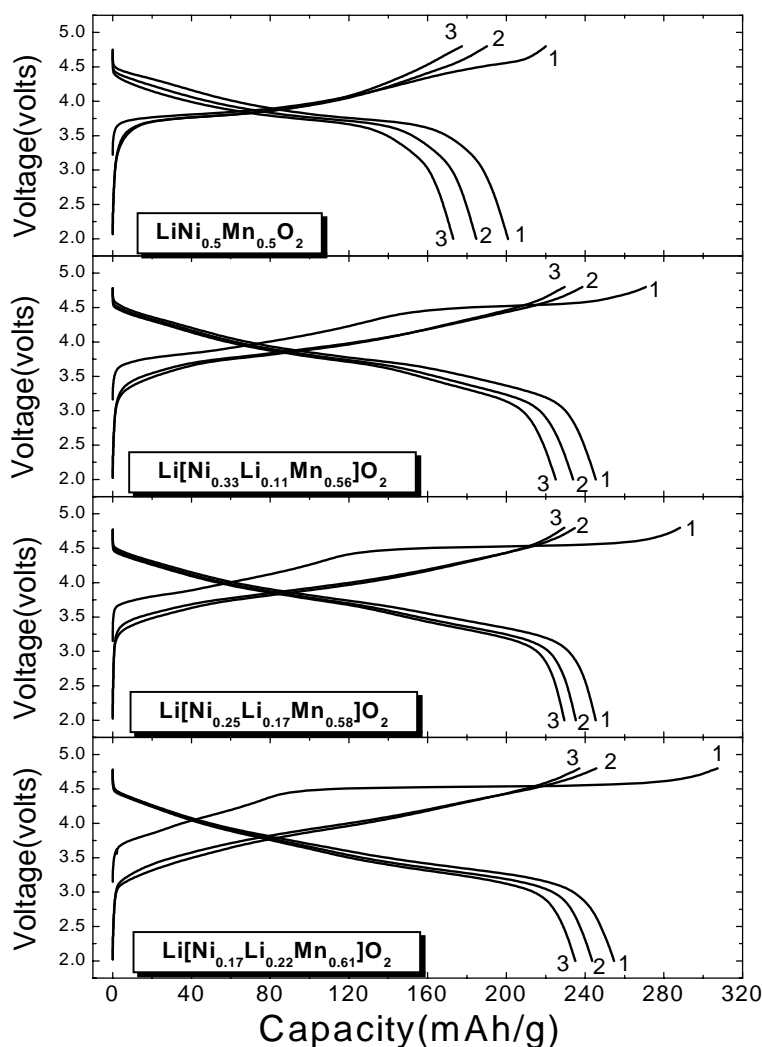


Fig. 4. First three charge–discharge profiles for $\text{Li}[\text{Ni}_x\text{Li}_{(1/3-2x/3)}\text{Mn}_{(2/3-x/3)}]\text{O}_2$ ($x = 0.17, 0.25, 0.33, 0.5$) compounds between 4.8 and 2.0 V at constant current density of 20 mA g^{-1} .

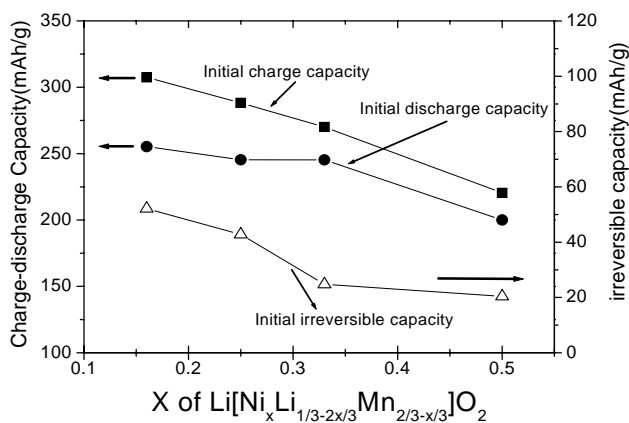


Fig. 5. Initial charge–discharge and irreversible capacity for $\text{Li}[\text{Ni}_x\text{Li}_{1/3-2x/3}\text{Mn}_{2/3-x/3}]\text{O}_2$ ($x = 0.17, 0.25, 0.33, 0.5$) compounds. Voltage range and constant current density are 4.8–2.0 V and 20 mA g^{-1} , respectively.

the plateau at about 4.5 V corresponds to the removal of the remaining lithium from the lithium layer, along with the simultaneous ejection of oxygen. By contrast, Robertson and Bruce [22] have concluded that the exchange of Li^+ by

H^+ in non-aqueous media results in a long and irreversible plateau. The initial discharge capacity of the compounds increases from 200 to 255 mAh g^{-1} with decrease in Ni content. The $\text{Li}[\text{Ni}_{0.50}\text{Mn}_{0.50}]\text{O}_2$ compound delivers a relatively low initial discharge capacity of about 200 mAh g^{-1} . On the other hand, the remaining compounds give very high initial discharge capacity of over 245 mAh g^{-1} .

The cycle performance of cells with $\text{Li}[\text{Ni}_x\text{Li}_{1/3-2x/3}\text{Mn}_{2/3-x/3}]\text{O}_2$ cathode materials at 21°C is presented in Fig. 6. The current density and the voltage range are 20 mA g^{-1} and 4.8–2.0 V, respectively. $\text{Li}[\text{Ni}_{0.17}\text{Li}_{0.22}\text{Mn}_{0.61}]\text{O}_2$ and $\text{Li}[\text{Ni}_{0.25}\text{Li}_{0.17}\text{Mn}_{0.58}]\text{O}_2$ compounds display very stable cycle performance. The discharge capacities of these compounds are sustained of about 200 mAh g^{-1} after the first several cycles. By contrast, the $\text{Li}[\text{Ni}_{0.33}\text{Li}_{0.11}\text{Mn}_{0.56}]\text{O}_2$ and $\text{Li}[\text{Ni}_{0.50}\text{Mn}_{0.50}]\text{O}_2$ compounds show a relatively large loss in capacity on cycling.

The XRD analysis and electrochemical results suggest that the simple combustion method, is more appropriate for synthesizing $\text{Li}[\text{Ni}_x\text{Li}_{1/3-2x/3}\text{Mn}_{2/3-x/3}]\text{O}_2$ compounds with low Ni content ($x \leq 0.25$). In previous reports [18–21], $\text{Li}[\text{Ni}_x\text{Li}_{1/3-2x/3}\text{Mn}_{2/3-x/3}]\text{O}_2$ cathode material

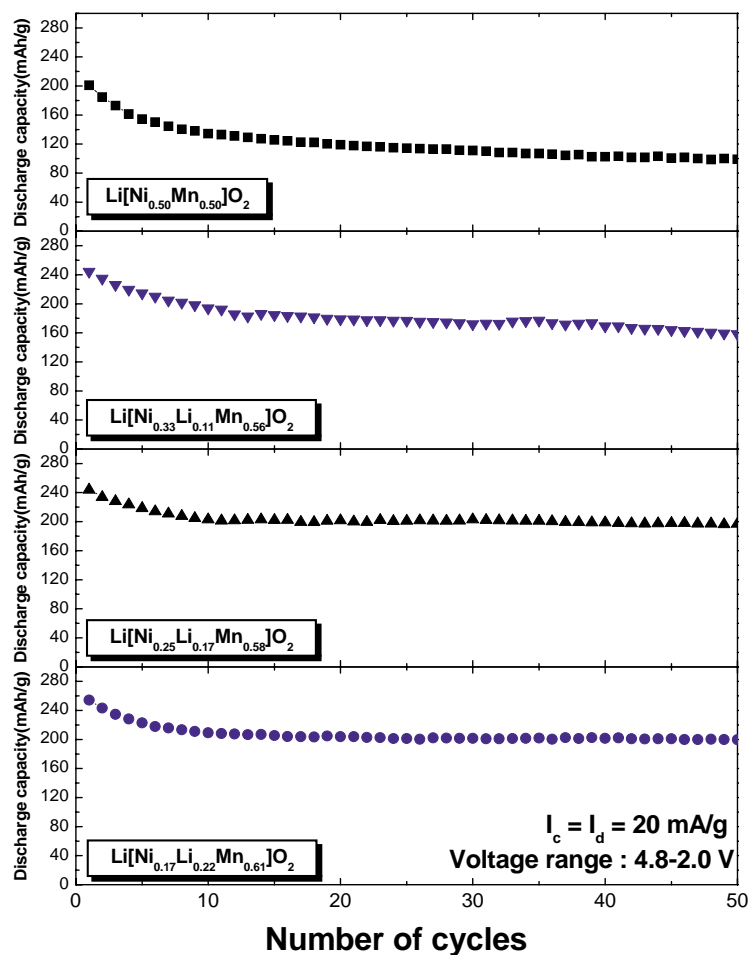


Fig. 6. Cycle performance of $\text{Li}[\text{Ni}_x\text{Li}_{1/3-2x/3}\text{Mn}_{2/3-x/3}]\text{O}_2$ ($x = 0.17, 0.25, 0.33, 0.5$) compounds between 4.8 and 2.0 V at constant current density of 20 mA g^{-1} .

prepared by a mixed hydroxide method has been reported. The mixed hydroxide method will lead to enhancement in homogeneity of cation ($M = \text{Mn}, \text{Ni}, \dots$), but it requires a rather complex synthetic process. With respect to industrial applications, it is very important to simplify the synthetic procedure in order to minimize the cost of manufacture. Synthesized through a simple combustion method, $\text{Li}[\text{Ni}_{0.50}\text{Mn}_{0.50}]\text{O}_2$ and $\text{Li}[\text{Ni}_{0.33}\text{Li}_{0.11}\text{Mn}_{0.56}]\text{O}_2$ compounds appeared to have a mixed phase and show unstable cycle performances. However, in terms of discharge capacity and cycle life, the $\text{Li}[\text{Ni}_{0.17}\text{Li}_{0.22}\text{Mn}_{0.61}]\text{O}_2$ and $\text{Li}[\text{Ni}_{0.25}\text{Li}_{0.17}\text{Mn}_{0.58}]\text{O}_2$ compounds are as good as similar materials prepared by the mixed hydroxide method. As a consequence, $\text{Li}[\text{Ni}_x\text{Li}_{(1/3-2x/3)}\text{Mn}_{(2/3-x/3)}]\text{O}_2$ compounds with low Ni content ($x \leq 0.25$) can be successfully synthesized, not only by the complex mixed hydroxide method but also by the simple combustion method except for small amount of inhomogeneous cation-mixing. Thus, the latter method promises to be an effective means of reducing production cost.

The cyclic properties of $\text{Li}[\text{Ni}_{0.17}\text{Li}_{0.22}\text{Mn}_{0.61}]\text{O}_2$ and $\text{Li}[\text{Ni}_{0.25}\text{Li}_{0.17}\text{Mn}_{0.58}]\text{O}_2$ compounds measured at 21 and 30 °C as a function of current density are presented in Fig. 7. These compounds display a stable cycle performance at 20 mA g⁻¹ (see Fig. 6). The cell is initially charged

and discharged with a current density of 20 mA g⁻¹ (about 0.1 C rate) between 4.8 and 2.0 V. After the initial five cycles, the current density is increased to 40 mA g⁻¹ for an additional 20 cycles. Current densities of 100 (about 0.5 C rate) and 200 mA g⁻¹ (about 1 C rate) are adopted in succession for the subsequent 20 cycles. The discharge capacity is decreased to below 60% of the 5th cycle as the current density is increased to 200 mA g⁻¹, but the cycle does not deteriorate. It is interesting that the discharge capacity measured at 30 °C is higher than that at 21 °C, i.e., by about 10–20 mAh g⁻¹. It is clear that a small increase in test temperature results in a considerable enhancement in discharge capacity at different specific current densities.

4. Conclusions

$\text{Li}[\text{Ni}_x\text{Li}_{(1/3-2x/3)}\text{Mn}_{(2/3-x/3)}]\text{O}_2$ ($x = 0.17, 0.25, 0.33, 0.5$) powders have been synthesized by a simple combustion method. Compounds with low Ni content show better phase integrity than those with high Ni content. The specific capacity of these materials is 200–255 mAh g⁻¹ in the initial cycle between 4.8 and 2.0 V. The lower Ni contents in the samples results in an enhancement in charge–discharge capacity and initial irreversible capacity. $\text{Li}[\text{Ni}_{0.17}\text{Li}_{0.22}\text{Mn}_{0.61}]\text{O}_2$ and $\text{Li}[\text{Ni}_{0.25}\text{Li}_{0.17}\text{Mn}_{0.58}]\text{O}_2$ display a very stable cycle performance and a sustained high discharge capacity of about 200 mAh g⁻¹ after several cycles. By contrast $\text{Li}[\text{Ni}_{0.50}\text{Mn}_{0.50}]\text{O}_2$ compound suffers an abrupt capacity loss during cycling. The XRD analysis and electrochemical results suggest that the simple combustion method is more appropriate for synthesizing $\text{Li}[\text{Ni}_x\text{Li}_{(1/3-2x/3)}\text{Mn}_{(2/3-x/3)}]\text{O}_2$ compounds with low Ni content ($x \leq 0.25$).

Acknowledgements

This work was supported by the Korea Ministry of Information and Communication (MIC) (No. 2003-S-003).

References

- [1] T. Nagaura, K. Tozawa, *Prog. Batteries Sol. Cells* 9 (1990) 209.
- [2] K. Mizushima, P.C. Jones, P.J. Wiseman, J.B. Goodenough, *Mater. Res. Bull.* 15 (1980) 783.
- [3] D.D. MacNeil, Z. Lu, J.R. Dahn, *J. Electrochem. Soc.* 149 (10) (2002) A1332.
- [4] A.R. Armstrong, P.G. Bruce, *Nature* 381 (1996) 499.
- [5] A.R. Armstrong, B. Haug, R.A. Jennings, P.G. Bruce, *J. Mater. Chem.* 8 (1998) 255.
- [6] Y. Shao-Horn, S.A. Hackney, A.R. Armstrong, P.G. Bruce, R. Gitzendanner, C.S. Johnson, M.M. Thackeray, *J. Electrochem. Soc.* 146 (1999) 2404.
- [7] R.J. Gummow, M.M. Thackeray, *J. Electrochem. Soc.* 141 (1994) 1178.
- [8] Y. Jang, B. Haug, H. Wang, D. Sadoway, Y. Chiang, *J. Electrochem. Soc.* 146 (1999) 3217.

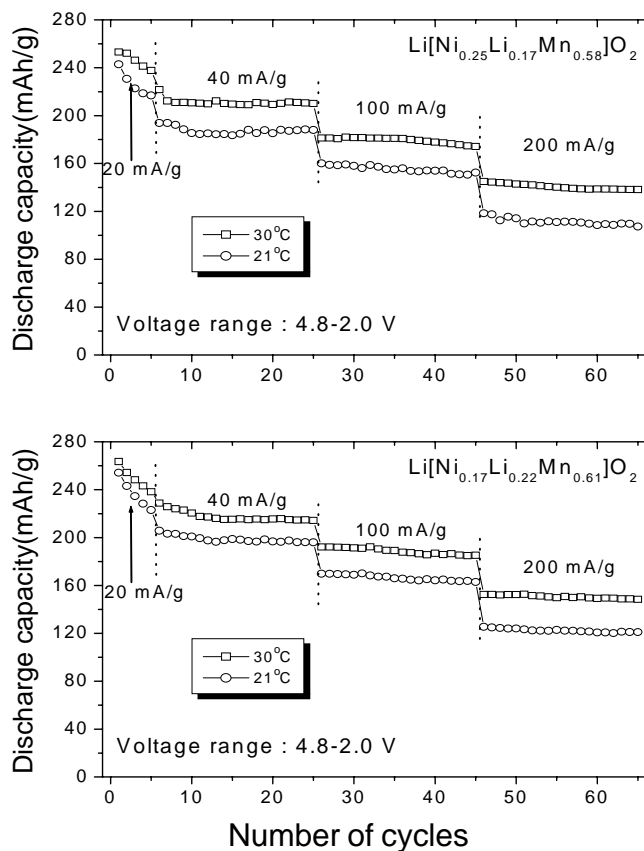


Fig. 7. Cycle performance of $\text{Li}[\text{Ni}_{0.17}\text{Li}_{0.22}\text{Mn}_{0.61}]\text{O}_2$ and $\text{Li}[\text{Ni}_{0.25}\text{Li}_{0.17}\text{Mn}_{0.58}]\text{O}_2$ compounds at 21 and 30 °C as function of constant current density in voltage range 4.8–2.0 V.

- [9] B. Ammundsen, J. Desilvestro, T. Groutso, D. Hassell, J.B. Metson, E. Regan, R. Steiner, P.J. Pickering, *J. Electrochem. Soc.* 147 (2000) 4078.
- [10] J. Reed, G. Ceder, A. Van Der Ven, *Electrochem. Solid-State Lett.* 4 (2001) A78.
- [11] J.R. Dahn, T. Zheng, C.L. Thomas, *J. Electrochem. Soc.* 145 (1998) 851.
- [12] J. Cho, B. Park, *Electrochem. Solid-State Lett.* 3 (2000) 355.
- [13] J. Cho, Y.J. Kim, B. Park, *Solid State Ionics* 138 (2001) 221.
- [14] J.M. Paulsen, B. Ammundsen, H. Desilvestro, R. Steiner, D. Hassell, Abstract 71, The Electrochemical Society Meeting Abstracts, vol. 2000-2, Phoenix, AZ, 22–27 October 2000.
- [15] K. Numata, C. Sakaki, S. Yamanaka, *Chem. Lett.* (1997) 725.
- [16] K. Numata, C. Sakaki, S. Yamanaka, *Solid State Ionics* 117 (1999) 257.
- [17] Z. Lu, D.D. MacNeil, J.R. Dahn, *Electrochem. Solid-State Lett.* 4 (11) (2001) A191.
- [18] Z. Lu, L.Y. Beaulieu, R.A. Donabarger, C.L. Thomas, J.R. Dahn, *J. Electrochem. Soc.* 149 (6) (2002) A778.
- [19] Z. Lu, J.R. Dahn, *J. Electrochem. Soc.* 149 (11) (2002) A1454.
- [20] Z. Lu, J.R. Dahn, *J. Electrochem. Soc.* 149 (7) (2002) A815.
- [21] Z. Lu, D.D. MacNeil, J.R. Dahn, *Electrochem. Solid-State Lett.* 4 (12) (2001) A200.
- [22] A.D. Robertson, P.G. Bruce, *Chem. Commun.* 2790 (2002).